Chapter 1: Introduction

"There is plenty of room at the bottom."

~Richard P. Feynman (Dec, 1959)

1.1 Overview of quantum confined materials

The term 'quantum confinement' describes the phenomenon that occurs when the dimensions of a material are reduced to the nanoscale, typically below its exciton Bohr radius [1–4]. In the case of two-dimensional (2D) materials, quantum confinement occurs along the out-of-plane direction, while charge carriers remain free to move in the other two in-plane directions [5–8]. This reduced dimensionality leads to a significant alteration in the electronic, optical, and vibrational properties of the material [9, 10]. As the material is thinned down to a few atomic layers, or even a single monolayer, the energy bands become discretized along the perpendicular reciprocal space direction, enhancing quantum effects and introducing phenomena that are not observed in their bulk counterparts. This unique confinement, combined with the high surface-to-volume ratio and symmetry-breaking effects, results in a wide range of novel physical behaviours such as tunable bandgaps, enhanced carrier mobility, and strong light-matter interactions.

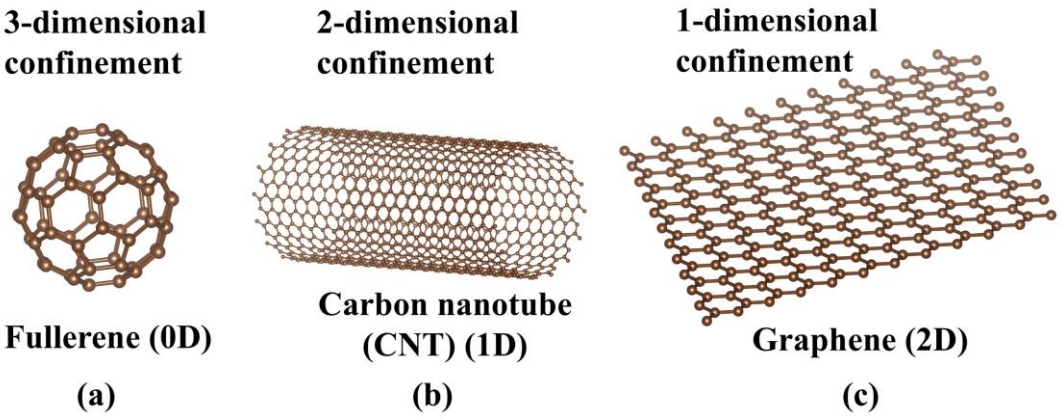

Figure 1.1: *Different allotropes of carbon-based quantum confined material.*

The realization of these extraordinary properties began with the groundbreaking discovery of graphene in 2004 by Andre Geim and Konstantin Novoselov, who mechanically exfoliated a single layer of carbon atoms from graphite [11]. Graphene, a honeycomb lattice of carbon atoms, possesses outstanding electrical conductivity, tensile strength, and thermal conductivity [12, 13]. Its groundbreaking properties sparked intense global interest and rapidly accelerated research into 2D materials. As researchers soon realized that

graphene was only the tip of the iceberg, a broader field of 2D materials emerged. In 2005, hexagonal boron nitride (*h*-BN), a compound composed of boron and nitrogen atoms in a similar honeycomb structure, was also successfully exfoliated and characterized [14]. *h*-BN stands out for its high thermal and chemical stability, making it a versatile material for various applications [14–16].

The momentum continued with the discovery of silicene in 2010, a monolayer of silicon atoms arranged in a graphene-like structure [17]. Silicene showed promise due to its intriguing electrical and optical properties [18, 19]. That same year marked another significant breakthrough with the discovery that monolayer molybdenum disulfide (MoS_2) possesses a direct semiconducting bandgap [20–22]. This finding not only enabled the development of 2D materials for electronics, optoelectronics, and catalysis, but also ushered in a new era focused on the transition metal dichalcogenide (TMDC) family [23].

TMDCs have the general chemical formula MX_2, where M is a transition metal (e.g., Mo, W, Nb, Ta) and X is a chalcogen (S, Se, or Te). These materials form layered structures held together by weak van der Waals (vdW) forces, allowing exfoliation down to monolayers. Depending on the specific combination of metal and chalcogen, TMDCs can exhibit semiconducting, metallic, or even superconducting behaviour, making them highly tunable for diverse applications [23, 24]. Following MoS_2, several other TMDCs were successfully exfoliated and studied. In 2012, monolayer molybdenum diselenide ($MoSe_2$) was reported, showing a direct bandgap and strong photoluminescence [25]. Around 2012-2013, tungsten diselenide (WSe_2) was isolated and recognized for its semiconducting nature and robust excitonic effects [26]. In 2013, tungsten disulfide (WS_2) gained attention due to its pronounced spin-orbit coupling and strong optical response [27]. Subsequently, in 2014, molybdenum ditelluride ($MoTe_2$) was introduced as a near-infrared semiconductor with tunable structural phases, expanding the spectral range of 2D optoelectronics [28].

1.2 Black Phosphorene and its analogous 2D materials

In this thesis, the primary focus shifts toward another emerging class of 2D materials, black phosphorous and its isostructural counterpart, tin(II) sulfide (SnS), which belong to the transition metal monochalcogenide (TMMC) family. The first successful exfoliation of monolayer black phosphorous, also known as black phosphorene (BP) was

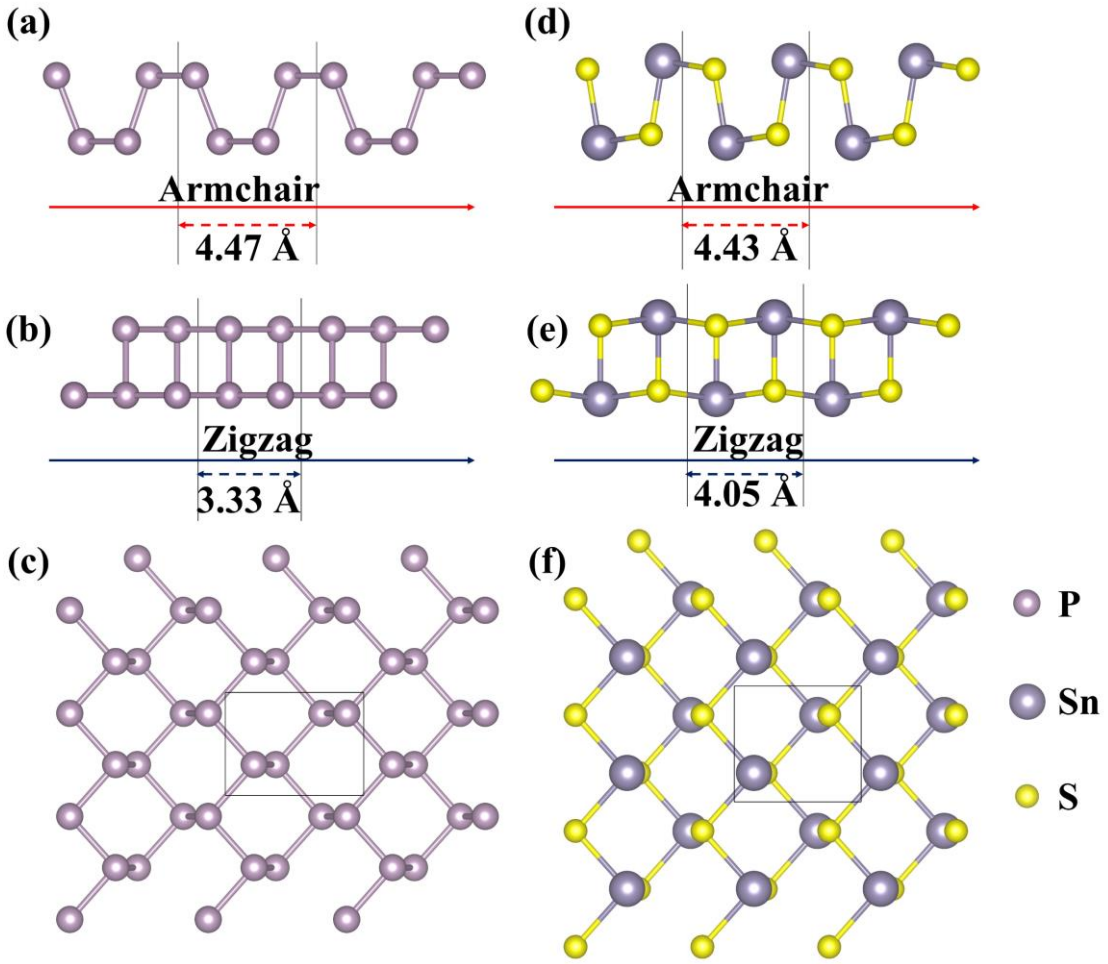

Figure 1.2: *Optimized geometrical structures of (a-c) BP and (d-f) SnS monolayers (3×3 supercell). Panels (a) and (d), and (b) and (e) show side views along the armchair and zigzag directions, respectively, while panels (c) and (f) present the top views.*

reported in 2014, demonstrating a direct bandgap and high hole mobility, which sparked widespread interest for its potential in next-generation nano electronic devices [29, 30]. Following this, SnS began to attract attention as a 2D material due to its structural and electronic similarities to BP [31]. Like BP, SnS is a group IV–VI compound with a puckered orthorhombic structure and pronounced in-plane anisotropy, making it a promising candidate for optoelectronic and thermoelectric applications [32–35]. The first successful isolation of SnS nanosheets was reported by Brent *et al.* in 2015 [36]. They employed liquid-phase exfoliation to produce SnS nanosheets with an average thickness corresponding to 3-4 bilayers. This pioneering work demonstrated the potential of SnS as a two-dimensional material with promising electronic and optical properties.

Unlike the three-atom-thick hexagonal structure of TMDC monolayers, BP and SnS are composed of two atomic layers and adopt an orthorhombic crystal structure. This class of materials has garnered considerable attention due to their inherent in-plane anisotropy and distinctive physicochemical characteristics [37]. The anisotropy arises from their puckered structural geometry, which creates two non-equivalent in-plane orthogonal lattice parameters, commonly referred to as the armchair (ac) and zigzag (zz) axes. The monolayer unit cell comprises four atoms, each covalently bonded to three neighbours, forming zigzag rows of alternating elements. Lone pairs on each atom push the bonds into tetrahedral coordination, resulting in two short in-plane bonds and one long out-of-plane bond. This unique geometry creates pronounced anisotropy along the ac and zz directions [38, 39]. The structural anisotropy of BP and SnS monolayer along with their lattice parameters are shown in Fig. 1.2 [40, 41]. Notably, in BP, all four atoms in the unit cell are phosphorus (P), whereas in monolayer SnS, the unit cell comprises two tin (Sn) and two sulfur (S) atoms, positioning it as a key representative of the TMMC family.

1.3 Motivation

1.3.1 Defect engineering: the concept of compound defect

Defects in quantum-confined materials play a pivotal role in tailoring their properties for a wide range of applications. These defects can originate intrinsically, due to lattice imperfections, or extrinsically, through external processing methods [42]. The strategic manipulation of these imperfections, commonly referred to as defect engineering, enables precise control over the electronic, optical, mechanical, and chemical behaviour of materials [43–46]. Defects in materials are commonly classified into categories such as point defects, line defects, grain boundaries, and other forms of extended structural irregularities [47].

Point defects such as vacancies and interstitials can introduce localized electronic states within the band structure, significantly affecting electrical conductivity, carrier mobility, and chemical reactivity [48–50]. Dislocations, also known as line defects, can alter mechanical properties and are instrumental in engineering materials for desired deformation behaviour [51]. Similarly, grain boundaries can influence charge and heat transport, thereby affecting the thermal and electrical conductivity of the material. Substitutional doping, wherein host atoms are replaced with foreign elements, allows for

precise tuning of the band structure and electronic properties [52–56]. Additionally, ad-atoms can modify the surface reactivity and interaction dynamics, offering new pathways for catalytic or sensing applications [57, 58].

To achieve desired properties, doping is a widely employed technique, particularly in 2D materials like graphene, TMDCs, and BP [59, 60]. In this context, n-type and p-type doping serve as essential strategies for tuning charge carrier concentrations. n-type doping introduces donor atoms, which contribute extra electrons, thereby increasing electrical conductivity and electron mobility. These dopants can either substitute host atoms or adsorb onto the surface. In contrast, p-type doping introduces acceptor atoms, that create holes, enhancing hole mobility. p-type behaviour is typically achieved by substituting atoms in the lattice or creating controlled vacancies. The choice and concentration of dopants significantly affect electrical, optical, thermal, and mechanical properties, making doping a central aspect of defect engineering [61–63].

Among intrinsic point defects, vacancies are especially impactful in 2D systems [64, 65]. Vacancies can form during exfoliation, fabrication, or under external stimuli like temperature fluctuations and chemical treatments. Vacancies introduce local lattice distortions and strain fields, which alter the mechanical strength, flexibility, and response to external forces. Electronically, they contribute to mid-gap defect states that influence conductivity, carrier mobility, and optical absorption [48, 49, 66, 67].

It is important to note that in recent years, extensive research on defect-engineered materials has primarily focused on single-point defect models, where only one type of defect, such as a vacancy or a dopant, is considered. However, in practical scenarios, there

Table 1.1: Vacancy formation energies of BP, graphene, silicene, WSe_2, and SnS.

Materials	Single vacancy (eV)	Double vacancy (eV)	References
BP	1.51-1.63	1.91-3.04	[40, 42]
Graphene	7.80	7.52	[42]
Silicene	3.77	3.70	[42]
WSe_2	5.30 (W)	-	[68]
	2.63 (Se)	-	
SnS	4.75 (Sn)	-	[69]
	6.03 (S)	-	

is a strong likelihood that multiple types of defects coexist within a single material. For example, the above table (Table 1.1) compares the vacancy formation energies of BP and SnS with other 2D materials such as graphene, silicene, and the TMDC material WSe_2. It is evident that the energy required to form single or double vacancies in BP is significantly lower compared to these other 2D systems. This suggests that vacancies are an inevitable feature of BP, and may naturally arise during exfoliation or any other growth process. Consequently, any study involving BP should carefully consider the likely presence and effects of such vacancies, as they can critically influence the physiochemical characteristics of the material.

Now, if BP is doped with foreign elements such as O, N, S, Al, etc., the material can simultaneously host both a dopant atom and a vacancy, resulting in existence of two different point defects. This specific combination of multiple defect types within a single host material is referred to as a 'compound defect'. The formation likelihood, stability, and influence of such a compound defect on the structural and electronic properties of BP are thoroughly examined in Chapter 3 of this thesis.

1.3.2 Surface adsorption phenomena

A particularly valuable outcome of defect engineering is the enhancement of surface reactivity. Defects such as vacancies or dopant sites act as active centres for gas adsorption, significantly improving the sensitivity and selectivity of materials in gas sensing applications. Given the vacancy-prone nature of BP, it has been extensively studied for toxic gas molecule adsorption using single-point defect models. For example, Kaewmaraya *et al.* showed that vacancies in BP substantially enhance its sensitivity to H_2S and SO_2 molecules [70]. Similarly, studies by Meshginqalam *et al.* demonstrated that vacancy formation increases the adsorption energies for NO_x and SO_x molecules in BP [71].

On the other hand, dopants also introduce defect sites, often enhancing surface reactivity. In this context, Suvansinpan *et al.* investigated BP doped with seventeen different elements, concluding that doping enhances chemical activity for nitrogen-based gas adsorption via electronic hybridization and charge transfer mechanisms [52]. In essence, the adsorption of target gas molecules at these defect sites can lead to measurable changes in electrical or optical signals, making defect-engineered BP ideal for next-generation sensors [49, 71–75].

Interestingly, when multiple defect types, such as a vacancy and a dopant atom, coexist within the same host material, forming a compound defect, their collective influence on the physicochemical properties of BP remains largely underexplored. Understanding the influence of such complex defects is especially important for surface-related applications, as they can further enhance surface reactivity and introduce additional dangling bonds, enabling stronger and more selective interactions with external molecules. This makes compound defects particularly attractive for catalysis, chemical sensing, and surface functionalization. The impact of such a compound defect is comprehensively investigated in Chapter 4 of this thesis, focusing on the surface adsorption of five environmentally detrimental gas molecules, and highlighting their potential in environmental monitoring and sensing technologies.

1.3.3 Heterostructure engineering: mixed-phase and mixed-dimensional systems

Heterostructure engineering refers to the strategic stacking or integration of different materials to tailor and combine their distinct physical, chemical, or electronic properties into a single functional system. In the context of 2D materials, where layers can be as thin as a single atomic sheet, this concept becomes particularly influential. By vertically or laterally assembling atomically thin materials with varying band structures, carrier mobilities, optical responses, and lattice symmetries, one can construct custom-designed platforms exhibiting emergent properties that are not present in the individual components [76–79].

This thesis focuses on two 2D materials: BP and SnS. BP is prone to defect formation, particularly vacancies, which although often seen as detrimental, can in fact enhance surface interactions. This makes BP an attractive candidate for gas sensing applications, where defect-mediated adsorption plays a vital role. On the other hand, SnS stands out for its excellent optoelectronic properties and has been extensively explored in photovoltaic and photo-detection applications. Unlike BP, SnS is significantly more stable with respect to vacancy formation (refer to Table 1.1), making it a robust platform for optoelectronic devices via heterostructure engineering.

1.3.3.1 Mixed-phase or isotropic-anisotropic heterostructures

In terms of optoelectronic properties, Maity *et al.* (2021) theoretically investigated excitonic behaviour in a SnS/GeSe heterostructure and found that its type-II band

alignment facilitates the formation of anisotropic interlayer excitons [80]. These excitons exhibit spatial separation of charge carriers across the two different layers, significantly prolonging their recombination lifetime, which in turn enhances the photovoltaic performance of SnS-based devices. This heterostructure was later experimentally realized by Sutter *et al.* in 2023 [81]. In recent years, various SnS-based heterostructures, formed by stacking SnS with materials such as BP, GeS, SnSe, etc., have been explored both theoretically and experimentally, showing potential across a range of applications [32, 35, 82–86]. It should be mentioned that SnS heterostructures based on similar lattice structures are extensively studied, but those with dissimilar lattices (orthorhombic-hexagonal) remain relatively underexplored, yet offer promising avenues for the development of mixed-phase heterostructures. One of the primary challenges in modelling such dissimilar systems arises from their high lattice mismatches and angular disparities. Furthermore, most hexagonal 2D materials, such as *h*-BN, MoS_2, $MoSe_2$, WS_2, WSe_2, and $MoTe_2$ exhibit in-plane isotropic optical and electronic properties [87–90]. In contrast, SnS, owing to its puckered orthorhombic crystal structure, displays in-plane anisotropy [41]. This makes one such orthorhombic-hexagonal heterostructure also an in-plane anisotropic/isotropic heterostructure. An in-plane isotropic nature leads to the quasi-2D particles, whereas, an anisotropic nature leads to quasi one-dimensional (1D) particles [91]. Hence, in-plane anisotropic/isotropic 2D heterostructures lead to the formation of quasi-1D/2D particle systems allowing for the manipulation of high binding energy quasi-1D particle populations. These systems are particularly advantageous for advanced optoelectronic applications, offering tunable properties that are difficult to achieve in conventional heterostructure with similar lattices. In Chapter 5 of this thesis, one such mixed-phase anisotropic/isotropic heterostructure is investigated as a strategic approach to enhance the optoelectronic performance of SnS-based devices.

1.3.3.2 Mixed-dimensional heterostructures

vdW interactions are not limited to interplanar forces in layered materials; rather, any passivated, dangling-bond-free surface can interact with another through vdW forces. This fundamental property allows layered 2D materials to be integrated with a wide variety of materials of differing dimensionalities, giving rise to mixed-dimensional vdW heterostructures. These combinations, involving 2D + nD (where n = 0, 1, or 3) materials, have emerged as a broad and versatile class of heterostructures, opening new avenues for material design and functional applications [92, 93].

Mixed-dimensional vdW systems are particularly compelling because they merge the quantum confinement effects of lower-dimensional materials with the planar charge transport properties of 2D materials. This synergy enhances light-matter interactions, carrier separation, and surface functionalization capabilities. For instance, CNT/WSe_2 mixed-dimensional heterostructures, with varying CNT chiralities, can significantly modulate band alignment and facilitate efficient exciton transfer, enabling exciton generation within CNTs [94]. Similarly, CNT-graphene heterostructures, formed via covalently bonded seamless junctions, can significantly reduce electrical and thermal contact resistance owing to their excellent electron and phonon transport properties [95].

The distinct confinement of charge carriers in each component contributes to novel physical behaviours, making these engineered systems highly promising for applications in optoelectronics, and energy harvesting. The interfacial charge dynamics and optoelectronic properties of an SnS-based 2D/1D mixed-dimensional heterostructure is extensively discussed in Chapter 6 of the thesis.

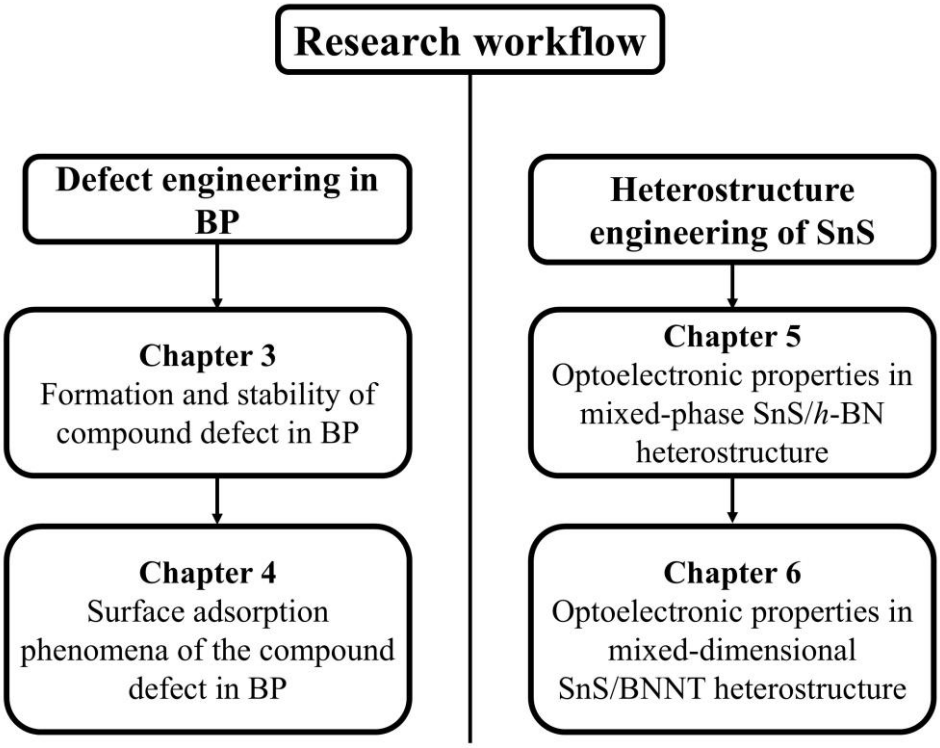

Figure 1.3: *Schematic overview of the research works presented in the thesis. Chapters 3 and 4 focus on defect engineering in BP, while Chapters 5 and 6 explore heterostructure engineering involving SnS-based systems.*

1.4 Objectives of the thesis

1. To model and study engineered BP and its isostructural SnS system, providing new perspective on their physiochemical properties using density functional theory (DFT).
2. To investigate the ground state geometrical structure, electronic and optical properties of the systems under consideration.
3. To explore the effect of external perturbation (e.g., strain, electric field, etc.) with a potential to tune the aforementioned properties of the systems.
4. To understand the correlation between the properties of the engineered materials and their potential applications (such as energy storage, gas sensor, etc.).
5. To strengthen our insight of the mechanisms involved in order to deepen current knowledge.

References

[1] Kis, A. 2D transition metal dichalcogenides. *Nature Reviews Materials*, 2(8): 1–15, 2017.

[2] Ramalingam, G., Kathirgamanathan, P. Quantum Confinement Effect of. *Quantum Dots: Fundamental and Applications*, 11, 2020.

[3] Dye, J. L. Electrides: early examples of quantum confinement. *Accounts of chemical research*, 42(10): 1564–1572, 2009.

[4] Takagahara, T., Takeda, K. Theory of the quantum confinement effect on excitons in quantum dots of indirect-gap materials. *Physical Review B*, 46(23): 15578, 1992.

[5] Mas-Balleste, R., Gomez-Navarro, C., Gomez-Herrero, J., Zamora, F. 2D materials: to graphene and beyond. *Nanoscale*, 3(1): 20–30, 2011.

[6] He, F., Zhou, Y., Ye, Z., Cho, S. H., Jeong, J., Meng, X., Wang, Y. Moiré patterns in 2D materials: a review. *ACS nano*, 15(4): 5944-5958, 2021.

[7] Avouris, P., Heinz, T. F., Low, T. 2D Materials. Cambridge University Press, 2017.

[8] Zhang, H. Introduction: 2D materials chemistry. *Chemical reviews*, 118(13), 6089-6090, 2018.

[9] Yuan, J. Electromagnetic response and energy conversion for functions and devices in low-dimensional materials. *Advanced Functional Materials*, 29(25): 1807398, 2019.

[10] Liu, X., Guo, Q., Qiu, J. Emerging low-dimensional materials for nonlinear optics and ultrafast photonics. *Advanced Materials*, 29(14): 1605886, 2017.

[11] Geim, A. K., Novoselov, K. S. The rise of graphene. *Nature materials*, 6(3): 183–191, 2007.

[12] Mortazavi, B., Ahzi, S. Thermal conductivity and tensile response of defective graphene: A molecular dynamics study. *Carbon*, 63: 460–470, 2013.

[13] Javvaji, B., Mortazavi, B., Rabczuk, T., Zhuang, X. Exploration of mechanical, thermal conductivity and electromechanical properties of graphene nanoribbon springs. *Nanoscale Advances*, 2(8): 3394–3403, 2020.

[14] Geim, A. K. Two-dimensional atomic crystals. *Proceedings of the National Academy of Sciences*, 102(30): 10451–10453, 2005.

[15] Kostoglou, N., Polychronopoulou, K., Rebholz, C. Thermal and chemical stability of hexagonal boron nitride (h-BN) nanoplatelets. *Vacuum*, 112: 42–45, 2015.

[16] Li, L. H. High thermal conductivity of high-quality monolayer boron nitride and its thermal expansion. *Science advances*, 5(6): eaav0129, 2019.

[17] Le Lay, G. Graphene-like silicon nanoribbons on Ag (110): A possible formation of silicene. *Applied Physics Letters*, 96(18), 2010.

[18] Emami-Nejad, H., Mir, A., Farmani, A., Talebzadeh, R. Outstanding tunable electrical and optical characteristics in monolayer silicene at high terahertz frequencies. *Journal of Computational Electronics*, 21(3): 590–598, 2022.

[19] Le Lay, G. Silicene: compelling experimental evidence for graphenelike two-dimensional silicon. *Physical review letters*, 108(15): 155501, 2012.

[20] Kis, A. Single-layer MoS_2 transistors. *Nature nanotechnology*, 6(3): 147–150, 2011.

[21] Wang, F. Emerging photoluminescence in monolayer MoS_2. *Nano letters*, 10(4): 1271–1275, 2010.

[22] Heinz, T. F. Atomically thin MoS_2: a new direct-gap semiconductor. *Physical review letters*, 105(13): 136805, 2010.

[23] Miroshnichenko, A. E. Recent advances on strong light-matter coupling in atomically thin TMDC semiconductor materials. *Journal of Optics*, 24(5): 053001, 2022.

[24] Dong, R., Kuljanishvili, I. Progress in fabrication of transition metal dichalcogenides heterostructure systems. *Journal of Vacuum Science & Technology B*, 35(3), 2017.

[25] Wu, J. Thermally driven crossover from indirect toward direct bandgap in 2D semiconductors: $MoSe_2$ versus MoS_2. *Nano letters*, 12(11): 5576–5580, 2012.

[26] Eda, G. Evolution of electronic structure in atomically thin sheets of WS_2 and WSe_2. *ACS nano*, 7(1): 791–797, 2013.

[27] Yao, W. Optical signature of symmetry variations and spin-valley coupling in atomically thin tungsten dichalcogenides. *Scientific reports*, 3(1): 1608, 2013.

[28] Ruppert, C., Aslan, B., Heinz, T. F. Optical properties and band gap of single-and few-layer $MoTe_2$ crystals. *Nano letters*, 14(11): 6231–6236, 2014.

[29] Zhang, Y. Black phosphorus field-effect transistors. *Nature nanotechnology*, 9(5): 372–377, 2014.

[30] Ye, P. D. Phosphorene: an unexplored 2D semiconductor with a high hole mobility. *ACS nano*, 8(4): 4033–4041, 2014.

[31] Gomes, L. C., Carvalho, A. Phosphorene analogues: Isoelectronic two-dimensional group-IV monochalcogenides with orthorhombic structure. *Physical Review B - Condensed Matter and Materials Physics*, 92(8), 2015.

[32] Xie, H. Transport and Thermoelectric Properties of SnX (X = S or Se) Bilayers and Heterostructures. *ACS Applied Energy Materials*, 3(7): 6946–6955, 2020.

[33] He, W., Ang, R., Zhao, L. D. Remarkable electron and phonon transports in low-cost SnS: a new promising thermoelectric material. *Science China Materials*, 65(5): 1143–1155, 2022.

[34] Tritsaris, G. A., Malone, B. D., Kaxiras, E. Optoelectronic properties of single-layer, double-layer, and bulk tin sulfide: A theoretical study. *Journal of Applied Physics*, 113(23), 2013.

[35] Nguyen, C. V. First principles study of structural, optoelectronic and photocatalytic properties of SnS, SnSe monolayers and their van der Waals heterostructure. *Chemical Physics*, 539: 110939, 2020.

[36] O'Brien, P. Tin (II) sulfide (SnS) nanosheets by liquid-phase exfoliation of herzenbergite: IV–VI main group two-dimensional atomic crystals. *Journal of the American Chemical Society*, 137(39): 12689–12696, 2015.

[37] Su, J., Xiao, B., Jia, Z. A first principle study of black phosphorene/N-doped graphene heterostructure: Electronic, mechanical and interface properties. *Applied Surface Science*, 528: 146962, 2020.

[38] Zhang, M., Biesold, G. M., Lin, Z. A multifunctional 2D black phosphorene-based platform for improved photovoltaics. *Chemical Society Reviews*, 50(23): 13346–13371, 2021.

[39] Mohebbi, E., Seyyed Fakhrabadi, M. M. First-principles calculations to investigate strain-tunable electronic bandgap of black phosphorus-structured nitrogen with desirable optical and elastic properties. *Materials Science and Engineering B: Solid-State Materials for Advanced Technology*, 281: 115745, 2022.

[40] Talukdar, D., Mohanta, D., Ahmed, G. A. Nitrogen Doped Compound Defect in Black Phosphorene for Enhanced Gas sensing. *Surfaces and Interfaces*, 51: 104699, 2024.

[41] Talukdar, D., Mohanta, D., Ahmed, G. A. Enhancing the optoelectronic properties of SnS via mixed-phase heterostructure engineering. *Nanoscale*, 17(6): 3331–3340, 2025.

[42] Hu, W., Yang, J. Defects in phosphorene. *The Journal of Physical Chemistry C*, 119(35): 20474–20480, 2015.

[43] Terrones, M. Defect engineering of two-dimensional transition metal dichalcogenides. *2D Materials*, 3(2): 022002, 2016.

[44] Fal'ko, V. I. Optical identification using imperfections in 2D materials. *2D Materials*, 4(4): 045021, 2017.

[45] Ni, Z. Defect engineering in 2D materials: precise manipulation and improved functionalities. Research, 2019.

[46] Li, H. Surface defect engineering in 2D nanomaterials for photocatalysis. *Advanced Functional Materials*, 28(39): 1801983, 2018.

[47] Tilley, R. J. D. *Defects in solids*. John Wiley & Sons, 2008.

[48] Behera, S. K., Deb, P. First principle understanding on electronic and magnetic behaviour in vacancy induced black phosphorous monolayer. In *AIP Conference Proceedings*, volume 2276, pages 020021, 2020, AIP Publishing LLC

[49] Hussain, T. Drastic improvement in gas-sensing characteristics of phosphorene nanosheets under vacancy defects and elemental functionalization. *The Journal of Physical Chemistry C*, 122(35): 20186–20193, 2018.

[50] Liu, L. M. Structures, stabilities and electronic properties of defects in monolayer black phosphorus. *Scientific reports*, 5(1): 1–11, 2015.

[51] Zou, X., Liu, M., Shi, Z., Yakobson, B. I. Environment-controlled dislocation migration and superplasticity in monolayer MoS_2. *Nano Letters*, 15(5): 3495–3500, 2015.

[52] Zhang, Y. W. Substitutionally doped phosphorene: electronic properties and gas sensing. *Nanotechnology*, 27(6): 065708, 2016.

[53] Wang, S. First-principles study of methanol adsorption on heteroatom-doped phosphorene. *Chinese Chemical Letters*, 30(1): 207–210, 2019.

[54] Goulart, L., Fernandes, L. da S., dos Santos, C. L., Rossato, J. Electronic and structural properties of black phosphorene doped with Si, B and N. *Physics Letters A*, 383(32): 125945, 2019.

[55] Amornkitbamrung, V. Ultrahigh-sensitive gas sensors based on doped phosphorene: A first-principles investigation. *Applied Surface Science*, 497: 143660, 2019.

[56] Qin, Y., Wang, X. Experiments combined with first-principles calculations to compare the enhancement of Ag-doping and -functionalization on the sensing properties of two-dimensional SnS. *Physica E: Low-Dimensional Systems and Nanostructures*, 131: 114752, 2021.

[57] Tian, S., Deng, C., Tang, Y., Tang, Q. Effect of adatom doping on the electrochemical performance of 1T′-MoS_2 for oxygen reduction reactions. *The Journal of Physical Chemistry C*, 124(45): 24899–24907, 2020.

[58] Park, J. Adatom doping of transition metals in $ReSe_2$ nanosheets for enhanced electrocatalytic hydrogen evolution reaction. *ACS nano*, 14(9): 12184–12194, 2020.

[59] Wu, P. Controllable doping in 2D layered materials. *Advanced Materials*, 33(48): 2104942, 2021.

[60] Wang, D., Li, X. B., Sun, H.-B. Modulation doping: a strategy for 2D materials electronics. *Nano Letters*, 21(14): 6298–6303, 2021.

[61] Large, L. N., Bicknell, R. W. Ion-implantation doping of semiconductors. *Journal of Materials Science*, 2*:* 589–609, 1967.

[62] Takenobu, T. Electrochemically doped light-emitting devices of transition metal dichalcogenide monolayers. In *JSAP Annual Meetings Extended Abstracts The 79th JSAP Autumn Meeting 2018*, pages 1257, 2018. The Japan Society of Applied Physics.

[63] Zan, R., Altuntepe, A. Nitrogen doping of graphene by CVD. *Journal of Molecular Structure*, 1199: 127026, 2020.

[64] Shim, J. J. Vacancy designed 2D materials for electrodes in energy storage devices. *Chemical Communications*, 59(41): 6109–6127, 2023.

[65] Zhang, Y. Vacancy defects in 2D transition metal dichalcogenide electrocatalysts: From aggregated to atomic configuration. *Advanced Materials*, 35(50): 2206576, 2023.

[66] Hussain, T. Drastic Improvement in Gas-Sensing Characteristics of Phosphorene Nanosheets under Vacancy Defects and Elemental Functionalization. *Journal of Physical Chemistry C*, 122(35): 20186–20193, 2018.

[67] Huang, B. Electronic and magnetic properties of perfect, vacancy-doped, and nonmetal adsorbed $MoSe_2$, $MoTe_2$ and WS_2 monolayers. *Physical Chemistry Chemical Physics*, 13(34): 15546–15553, 2011.

[68] Deka, B., Talukdar, D., Mohanta, D. Effect of 60 MeV nitrogen ion irradiation on few layer WSe_2 nanosystems. *Nuclear Instruments and Methods in Physics Research Section B: Beam Interactions with Materials and Atoms*, 554: 165438, 2024.

[69] Ullah, H., Kim, H. J., Shin, Y. H. Influences of vacancy and doping on electronic and magnetic properties of monolayer SnS. *Journal of Applied Physics*, *124*(6), 2018.

[70] Hussain, T. Drastic improvement in gas-sensing characteristics of phosphorene nanosheets under vacancy defects and elemental functionalization. *The Journal of Physical Chemistry C*, 122(35): 20186–20193, 2018.

[71] Meshginqalam, B., Barvestani, J. Vacancy defected blue and black phosphorene nanoribbons as gas sensor of NO_x and SO_x molecules. *Applied Surface Science*, 526: 146692*,* 2020.

[72] Qin, Y., Wei, Z., Bai, Y. Effect of vacancy defects of SnS on gas adsorption and its potential for selective gas detection. *Vacuum*, 183: 109792, 2021.

[73] Ghashghaee, M., Ghambarian, M. Highly improved carbon dioxide sensitivity and selectivity of black phosphorene sensor by vacancy doping: A quantum chemical perspective. *International Journal of Quantum Chemistry*, 120(16): e26265, 2020.

[74] Shukla, A., Gaur, N. K. The influence of S vacancy on the adsorption of toxic gas molecules on SnS monolayer: A DFT study. *Physica E: Low-Dimensional Systems and Nanostructures*, 120: 114054, 2020.

[75] Jasmine, J. M., Aadhityan, A., Thiruvadigal, D. J. A first-principles study of C_{l2}, PH_3, AsH_3, BBr_3 and SF_4 gas adsorption on MoS_2 monolayer with S and Mo vacancy. *Applied Surface Science*, 489: 841–848, 2019.

[76] Duan, X. Van der Waals heterostructures and devices. *Nature Reviews Materials*, 1(9): 1–17, 2016.

[77] Novoselov, K. S., Mishchenko, A., Carvalho, A., Castro Neto, A. H. 2D materials and van der Waals heterostructures. *Science*, 353(6298): aac9439, 2016.

[78] Chen, M. Emerging of heterostructure materials in energy storage: a review. *Advanced Materials*, 33(27): 2100855, 2021.

[79] Duan, X. 2D heterostructures for ubiquitous electronics and optoelectronics: principles, opportunities, and challenges. *Chemical reviews*, 122(6): 6514–6613, 2022.

[80] Singh, A. K. Anisotropic Interlayer Exciton in GeSe/SnS van der Waals Heterostructure. *Journal of Physical Chemistry Letters*, 12(7): 1765–1771, 2021.

[81] Sutter, P., Komsa, H. P., Kisslinger, K., Sutter, E. Lateral Integration of SnS and GeSe van der Waals Semiconductors: Interface Formation, Electronic Structure, and Nanoscale Optoelectronics. *ACS Nano*, 17(10): 9552–9564, 2023.

[82] Chen, J.-L., Wang, X. X., Shi, L. J. Electric field controlled type-I and type-II conversion of BP/SnS van der Waals heterostructure. *Journal of Physics: Condensed Matter*, 33(26): 265301, 2021.

[83] Chen, J. Le, Du, J. X., Yang, J., Shi, L. J. Modulation of strain on electronic structure and contact type of BP/SnS van der waals heterostructure. *Journal of Physics D: Applied Physics*, 55(12): 2022.

[84] Chen, Z. Significant improvement in thermoelectric performance of SnSe/SnS via nano-heterostructures. *Physical Chemistry Chemical Physics*, 23(6): 3794–3801, 2021.

[85] Li, Y. Transport behavior and thermoelectric properties of SnSe/SnS heterostructure modulated with asymmetric strain engineering. *Computational Materials Science*, 207: 111271, 2022.

[86] Huang, Y. Complete Separation of Carriers in the GeS/SnS Lateral Heterostructure by Uniaxial Tensile Strain. *ACS Applied Materials and Interfaces*, 9(46): 40969–40977, 2017.

[87] Talukdar, D., Bora, S. S., Ahmed, G. A. Electronic, optical, and adsorption properties of Li-doped hexagonal boron nitride: a GW approach. *Physical Chemistry Chemical Physics*, 26(5): 4021–4028, 2024.

[88] Shan, J. Tightly bound trions in monolayer MoS_2. *Nature materials*, 12(3): 207–211, 2013.

[89] Rasmussen, F. A., Thygesen, K. S. Computational 2D materials database: electronic structure of transition-metal dichalcogenides and oxides. *The Journal of Physical Chemistry C*, 119(23): 13169–13183, 2015.

[90] Shan, J. Tightly bound excitons in monolayer WSe_2. *Physical review letters*, 113(2): 026803, 2014.

[91] Neupane, G. P., Zhou, K., Chen, S., Yildirim, T., Zhang, P., Lu, Y. In-plane isotropic/anisotropic 2D van der Waals heterostructures for future devices. *Small*, 15(11), 1804733, 2019.

[92] Zhang, Y. Graphene-based mixed-dimensional van der Waals heterostructures for advanced optoelectronics. *Advanced Materials*, 31(37): 1806411, 2019.

[93] Jariwala, D., Marks, T. J., Hersam, M. C. Mixed-dimensional van der Waals heterostructures. *Nature materials*, 16(2): 170–181, 2017.

[94] Okada, S. Resonant exciton transfer in mixed-dimensional heterostructures for overcoming dimensional restrictions in optical processes. *Nature communications*, 14(1): 8152, 2023.

[95] Yang, C. Y. Structures, properties, and applications of CNT-graphene heterostructures. *2D Materials*, 6(4): 042005, 2019.